II.4

ATOMIC HYDROGEN AS A MODEL DEFECT IN ALKALI HALIDES

J.M. Spaeth

Fachbereich 6, Experimentalphysik, Universität-GH-Paderborn
Warburger Str. 100, 4790 Paderborn, FRG

Abstract

The results of electron spin resonance (ESR) and electron nuclear double resonance (ENDOR) experiments on atomic hydrogen centres on interstitial sites and both cation and anion substitutional sites are reviewed. Recent developments of the theoretical interpretation of the electronic ground state include the extension of the covalency model discussed earlier for interstitial centres to a configuration mixing model taking also into account hydrogen vibrations and the distortion of the ion orbitals due to Coulomb interactions.

The nature of the optical absorption of interstitial centres is briefly discussed. It is shown that fluorescence emission does not only occur for interstitial centres in a mixed configuration with one I^- next (H_i^o(I)-centres)) as assumed for a long time. It was recently also observed in KI and all cesium halides. The relaxed excited state of H_i^o(I)-centres in KCl and RbCl could very recently be investigated by means of optically detected magnetic resonance (ODMR). First results are reported.

1. Introduction

Impurity centres containing atomic hydrogen in alkali halides have a very simple structure. The hydrogen atoms can be trapped either interstitially or substitutionally. For a study of the electronic ground state or optically excited states the hydrogen centres are model systems because of the very simple electronic structure - the hydrogen atom is indeed the most simple impurity possible with its only 1s electron. Therefore, one should be able to use the free hydrogen 1s wave function as a good starting

function for a perturbation treatment of the interactions between the impurity atom and the surrounding lattice, since a complete ab initio calculation of the complicated many particle problem, which the calculation of the electronic structure of a defect represents, is not yet possible. In that sense the hydrogen centres are simpler than the F centres and therefore I feel they deserve a particular interest.

Meanwhile, there is a considerable amount of both experimental and theoretical work available on atomic hydrogen centres in alkali halides, which one cannot all review in a short article, nor is it possible to compare with results in the alkaline earth fluorides. A first review was given by the author in 1972 at the Luminy Conference, where mainly results on the ground state of the interstitial centres were reviewed (1). I will therefore only very briefly mention the main features of the ground state of interstitial centres as a background for the recent results on the ground state of substitutional centres in the first part of that article. In the second part I will review recent experimental work on the optically excited states of interstitial centres. It will be shown that the ground state is highly localised and very much "hydrogen-like". The quantitative understanding of the electronic ground state seems very good now.

2. Electronic structure of the ground state

Fig. 1 shows the models of the interstitial and two types of substitutional hydrogen centres. Interstitial centres (H_i^o-centres) can be produced by photodecomposition of OH^- or SH^- centres at temperatures below about 80 K (2-5). Substitutional centres on cation sites can be produced from interstitial centres in crystals doped with divalent cations like Sr^{++} or Ca^{++} in order to provide the cation vacancies. Through thermal annealing at about 100 K the interstitial hydrogen atoms diffuse and get trapped at the cation vacancies ($H_{s,c}^o$-centres). These centres are stable up to approximately 160 K (6,7). However, the presence of divalent cation ions lowers the symmetry of the centre. The anion centres ($H_{s,a}^o$-centres) are produced by X-irradiation of U-centres (H_s^--centres) at 77 K (8). The number of centres could be enhanced by one order of magnitude by doping the crystals

with Ag^+ ions which act as electron traps (9). The centres are stable up to 145 K.

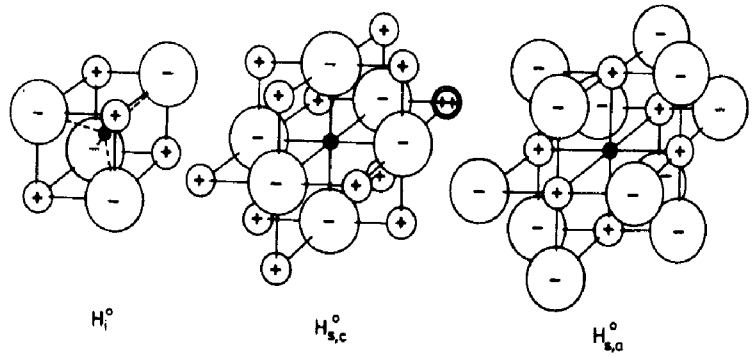

Fig. 1: Models of interstitial and substitutional atomic hydrogen centres in alkali halides.

The models of these centres are known from electron spin resonance (ESR) and above all from electron nuclear double resonance (ENDOR) measurements. Fig. 2 shows the ESR spectra of all these centres in KCl (10). The large splitting of about 500 G, which is nearly the same for all 3 centres, is due to the

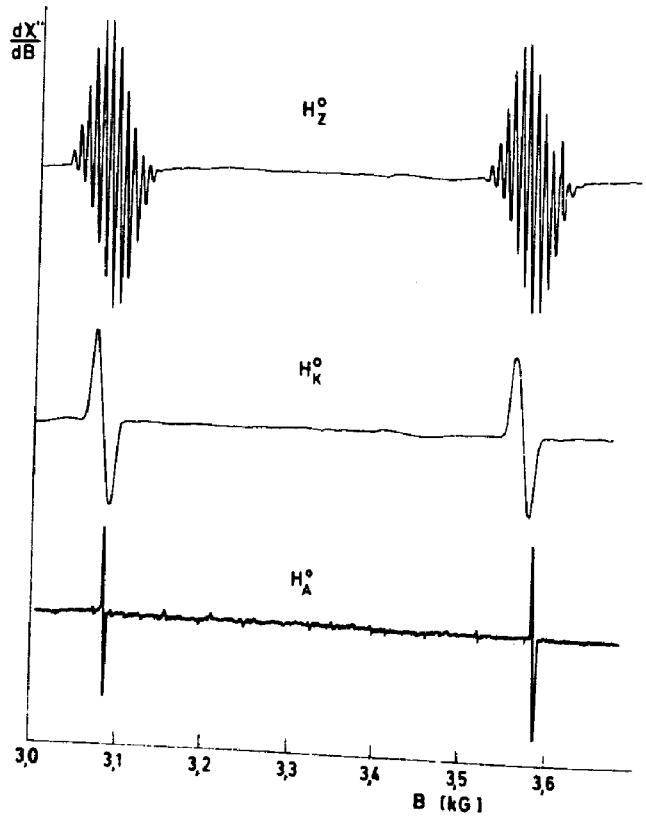

Fig. 2:
ESR spectra of 3 types of atomic hydrogen centres in KCl.

H_Z^O : interstitial centres;

H_K^O : hydrogen on cation sites (with Ca^{++} next in [110]);

H_A^O : hydrogen on anion sites.

$B_O \parallel [100]$, $\nu = 9.38 \cdot 10^9$ Hz, T = 80 K. (After [10]).

hyperfine interaction between the unpaired 1s electron and the proton, the two line groups correspond to the two possible orientations of the proton spin. The splitting is only about 1 to 3% smaller than that of the free hydrogen atom. This shows that the ground state of the hydrogen centres is very much hydrogen-like, the interactions with the lattice are only small. The additional splitting into 13 lines with a characteristic intensity ratio for the upper spectrum is due to superhyperfine (shf) interactions with the 4 nearest chlorine neighbours. From a comparison of such splittings in various alkali halides and their angular dependencies it could be concluded, that this spectrum is due to the interstitial centre (2,3). The other spectra show no additional shf structure, they differ only in the line width. Recently, with ENDOR experiments, the comparatively weak shf interactions could be resolved and it could be shown, that the spectrum with the larger line width is due to cation centres ($H^{O}_{s,c}$-centres) and the lowest one due to anion centres (6,7,9,11). For the interstitial centres ENDOR experiments not only confirmed the model derived from ESR, but the shf interactions with all nearest neighbours and several shells of neighbours in the further lattice surroundings could also be resolved (12,13). The main feature of the experimental result is that the spin density distribution $\psi^2(r)$ of the unpaired electron in the neighbourhood of the hydrogen atom is rather anisotropic in contrast to what one might expect from a spherically symmetric 1s function. This could be seen from the measured isotropic shf constants. The latter are related to the spin density $\psi^2(r)$ by

$$a_1 = \frac{2}{3}\,\mu_o g_I \mu_K g_e \mu_B |\psi(r_1)|^2 .$$

$\psi(r_1)$ is the centre electron wave function at the site of the nucleus 1 (g_e = electron g factor, g_I = nuclear g factor, μ_B = Bohr magneton, μ_K = nuclear magneton). Fig. 3 shows the positions of higher shell nuclei with respect to the hydrogen atom.Superhyperfine interactions could be resolved with first shell alkali and halogen neighbours, second shell alkali and halogen neighbours and third shell halogen neighbours. It is characteristic for the results that the unpaired spin density

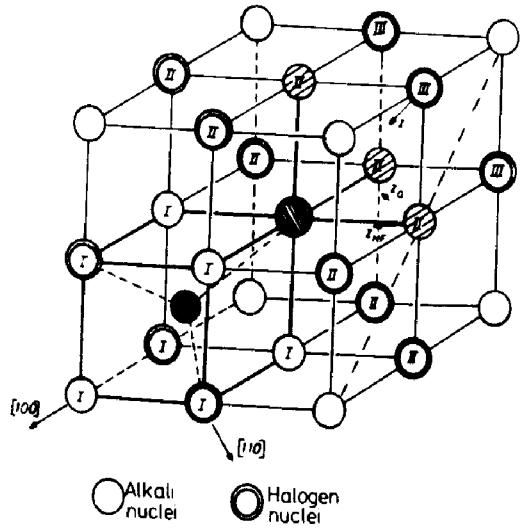

Fig. 3: Extended lattice surroundings of interstitial hydrogen centres in alkali halides.

at the first shell alkali neighbours is very low and that the alkali nuclei of the second shell show still a rather large unpaired spin density - its shf tensor is oriented in the connection line to the first halogen neighbours. The second shell halogen neighbours show only the classical dipole-dipole interaction. It looks as if the unpaired spin density is drawn towards the 4 nearest halogen neighbours and transferred from there further into the lattice. In KBr, e.g. $a(K^{II})$ is bigger than $a(K^{I})$! (12,13,14).

A theoretical explanation of these results was attempted with various theoretical approaches (see (1) for further references)). A rather good quantitative explanation of most of the experimental data was achieved with a theoretical model, which has the following main features (15):

i) The unperturbed hydrogen 1s function is used as envelope function.

ii) Löwdin orthogonalisation of the envelope function to the lattice ions (consideration of ion core overlaps). The orbitals of the free ions are taken.

iii) Small covalent bonding to nearest halogen neighbours.

iv) Consideration of zero point vibrations.

Through the orthogonalisation occupied neighbour ion orbitals are admixed into the hydrogen 1s function. The admixtures determine the order of magnitude of the observed shf constants. The consideration of the ion core overlaps qualitatively explains the anisotropy of the spin density distribution (12). The agreement with experiment was rather good when assuming in addition a small covalency admixture of nearest halogen outer p orbitals. The amount of covalency admixture, however, had to be determined semiempirically from the nearest halogen anisotropic shf interaction constant (15). A comparison between many alkali halides showed that the covalency parameters needed to explain the data are approximately proportional to the overlap integrals between the hydrogen 1s function and the halogen p functions (16).

A comparison of the shf interactions between the interstitial hydrogen and deuterium centres showed, that deuterium centres have smaller interactions. It turns out that a substantial fraction of the measured shf constants is due to zero point vibrations, that is purely dynamical in nature. In the experiment one observes an average over the fast vibrations ($\nu \sim 10^{13}$ Hz). The shf interactions depend via the overlap integrals exponentially on the distance between the hydrogen atom and the neighbours. By averaging over the Gaussian distribution of the hydrogen positions one can allow for the influence of the zero point vibrations on the shf interaction provided the frequency of that vibration is known (17). That was not the case at the time of the analysis of the ENDOR data. Instead, the isotope effect of the isotropic and anisotropic shf constants of the nearest halogen neighbours was used to determine this frequency. Unfortunately 2 frequencies were obtained differing by a factor of about 2. This showed that the theoretical model did not reliably explain either the isotropic or the anisotropic halogen interaction (16). It turned out later from results obtained for substitutional centres that the frequency obtained

from the anisotropic halogen interaction was the correct one, a result which was also confirmed by recent Raman measurements (18) and by infrared absorption, which could be observed in samples with a high concentration of centres necessary because of the small Szigeti charge of the nominally neutral centres (19). For KCl, e.g. from ENDOR one obtained ≈ 420 cm^{-1}, while both the Raman and IR measurements yielded 437 cm^{-1} and 441 cm^{-1}, respectively, in excellent agreement. Although the overall agreement with experiment obtained with this theoretical model was rather good, a few serious discrepancies remained, e.g., the spin density of the nearest halogens could not be explained satisfactorily (1,16).

A rather good further test for the simple theoretical model was its application to substitutional centres. They were investigated in recent years and show a number of additional features.

The shf interactions are a lot smaller than for the interstitial centres. The ENDOR spectra contain very many lines in a narrow frequency range making the analysis of the angular dependencies rather difficult and requiring the measurement of the full ENDOR spectrum for many small angular steps. For these experiments we used a computer controlled ENDOR spectrometer, which allowed fully automatic measurements including the rotation of the crystal and which allowed also the automatic determination of the line positions with the aid of a peak search algorithm (20). Fig. 4 shows the results for the anion centre in KCl as an example. In Fig. 4a the angular dependence of the ENDOR lines for rotation of the crystal in a (100) plane in steps of 1.08^{o} is shown as obtained from the computer controlled spectrometer. The sizes of the dots indicate the height of the corresponding lines. Fig. 4b shows the analysis of the angular dependence. The spin Hamiltonian was diagonalised numerically and the shf and quadrupole interaction parameters were fitted to the experiment with a special computer programme (11,20). The small points in the upper part of Fig. 4a are due to forbidden transitions with $\Delta m_I = \pm 2, \pm 3$. The shf and quadrupole interactions with 4 shells of neighbour ions could be determined with high precision.

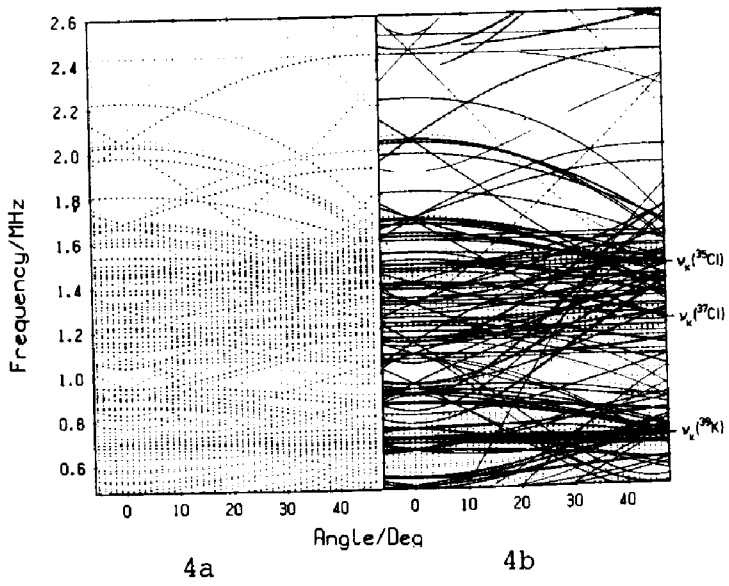

Fig. 4: Angular dependence of the ENDOR lines of $H^{O}_{s,a}$-centres in KCl. The crystal was rotated in a (001) plane. $O^{O} \hat{=} B_o \| [100]$; T = 40 K, B_o = 3514 G. a) Experimental results. b) Calculated angular dependence after determination of the spin Hamiltonian parameters of $^{39}K_I$, $^{35}Cl_{II}$, $^{37}Cl_{II}$, $^{35}Cl_{IV}$ and $^{39}K_V$ and comparison to the experimental results. (After [11]).

In contrast to the interstitial centres measured so far, the ENDOR lines of both substitutional types of hydrogen centres depend strongly on the temperature (6,11). Fig. 5 shows this for an ENDOR line of a second shell Cl neighbour of anion centres in KCl. With increasing temperature the ENDOR frequency increases, that is the shf interactions increase. For this example, the frequency increase between 31 and 127 K amounts to 106 kHz (11). This temperature dependence is due to thermal excitation of higher hydrogen vibration modes. In those the hydrogen atom overlaps more strongly with the neighbour ion orbitals and hence the shf interaction increases. The effect of the lattice expansion is approximately compensated by the increased ion vibration amplitudes, so that the observed frequency shift is practically due to the hydrogen vibrations alone (11,21). The analysis of the temperature dependence showed that within the temperature range of the stability of the centres only the first excited state is occupied measurably and that

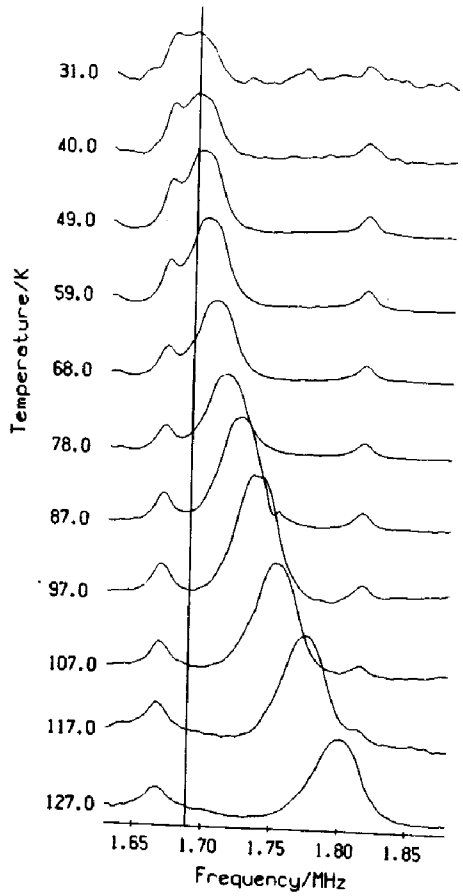

Fig. 5:

Temperature dependence of an ENDOR line of a second shell Cl neighbour of $H^{O}_{s,a}$-centres in KCl. (After [11]).

the vibrations can be described by a harmonic oscillator. The vibration frequency could be derived from the experimental temperature dependence of the shf interactions. All neighbours as well as the isotropic and anisotropic shf interaction parameters yield the same value for the vibration frequency. In KCl for $H^{O}_{s,a}$-centres 177 $\pm$8 cm^{-1}, for $H^{O}_{s,c}$-centres 199 $\pm$16 cm^{-1} were obtained, showing a much weaker vibrational potential compared to the interstitial centres. This frequency determination is independent of a particular model for the electronic structure of the centre. Therefore, the vibration potential can be used to calculate the shf interactions in a dynamical model.

When applying the theoretical model to anion centres one must take into account the lattice distortion around the anion vacancy. It was calculated using the HADES programme of Harwell (22,23,24) (see Fig. 6). The results for the shf constants are collected in table 1 in column "covalency". The model approximately explains the shf interactions of the potassium neighbours of the 1st and 5th shell and the anisotropic constant of the

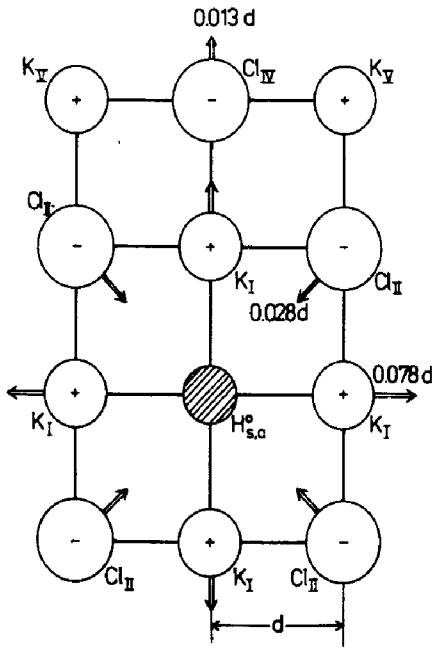

Fig. 6:

Location of the neighbours of anion centres in KCl and calculated lattice distortions. (After [11]).

4th shell Cl^- neighbours. Its value for the 2nd shell neighbours was fitted to determine the covalency parameters. Large discrepancies appear, however, especially for the isotropic shf constants of 2nd and 4th shell Cl neighbours, a qualitatively similar result as for interstitial centres. An additional chlorine s covalency is not improving the results, since then the isotope effect cannot be explained at the same time (24).

The theoretical interpretation of the shf interaction could be improved by taking into account two further refinements of the theoretical model:

i) distortion of the halogen orbitals by the positive charge of the anion vacancy,

ii) configuration mixing.

A perturbation calculation of the distorted Cl^- orbitals yields the following new Cl^- 3s and 3p functions:

$$\delta^{Cl^-}_{3s} = N_{3s}\left\{\psi^{Cl^-}_{3s} + \frac{e^2}{r^2}\sum_{n>3}\frac{\langle\psi^{Cl^-}_{np}|z|\psi^{Cl^-}_{3s}\rangle}{E_{3s}-E_{np}}\,\psi^{Cl^-}_{np}\right\},$$

$$\delta^{Cl^-}_{3p} = N_{3p}\left\{\psi^{Cl^-}_{3p} + \frac{e^2}{r^2}\sum_{n>3}\frac{\langle\psi^{Cl^-}_{ns}|z|\psi^{Cl^-}_{3p}\rangle}{E_{3p}-E_{ns}}\,\psi^{Cl^-}_{ns} + \frac{e^2}{r^2}\sum_{n>2}\frac{\langle\psi^{Cl^-}_{nd}|z|\psi^{Cl^-}_{3p}\rangle}{E_{3p}-E_{nd}}\psi^{Cl^-}_{nd}\right\}.$$

E_{ns}, E_{np} and E_{nd} are the energies of the states $\psi_{ns}^{Cl^-}$, $\psi_{np}^{Cl^-}$ and $\psi_{nd}^{Cl^-}$ respectively. N_{3s}, N_{3p} are normalisation constants.

An enhancement of spin density at the Cl^- sites is due to the fact that δ_{3p}, which is strongly admixed through the covalency does not vanish any more at the site of the Cl nucleus. The improvement is seen especially for Cl_{II} (table 1). Cl_{IV}, however, and the proton hyperfine interaction are still not well explained.

Table 1

Comparison of theoretical and experimental superhyperfine interactions of anion centres ($H^O_{s,a}$) in KCl.

		Experiment	Covalency	Distortion	Configuration
H^O	a_p(MHz)	1409.9	1419.7	1436.6	1417.1
K_I	a(kHz)	253	230	227	225
	b(kHz)	219	158	158	219*
Cl_{II}	a(kHz)	267	78	217	260
	b(kHz)	312	312*	312*	312*
Cl_{IV}	a(kHz)	37	3	5	30
	b(kHz)	54	36	36	47
K_V	a(kHz)	4	5	5	5
	b(kHz)	11	11	11	11

The values marked with asterisks were fitted to fix the covalency or configuration admixture coefficients.
a and b denote the superhyperfine interactions. (After [21,24]).

In the configuration mixing model one extends the simple covalency model to a many particle approach (25,26). Both models are equivalent if one neglects the difference between atomic and ionic orbitals (15). The configurations considered are $\psi_A = H^O - Cl^-_{II} - K^+_I$ and the two charge transfer configurations $\psi_B = H^- - Cl^O_{II} - K^+_I$ and $\psi_C = H^- - Cl^-_{II} - K^{++}_I$, in which outer p electrons are transferred to form H^-. The ground state is then

$$\psi = N\left\{\psi_A - \quad \mu\psi_B - \varepsilon\psi_C\right\}.$$

μ and ε are mixing parameters. The results obtained with this model are given in column "configuration" in table 1. μ and ε were fitted to explain the anisotropic shf constants of K_I and Cl_{II}. The exponent γ of the H^- orbital (the difference between the two orbitals in H^- was neglected) is also a free parameter and was chosen to be $\gamma = 0.31$, for which the agreement with the experiment was best. The overall agreement with experiment is very good now, also for the isotope effects not shown in table 1 (24). One special feature should be stressed: in the charge transfer state $H^- - Cl^-_{II} - K^{++}_I \quad K_I$ carries a positive charge which because of its small distance very efficiently distorts the Cl_{IV} ion core. The effect is stronger than that of the vacancy charge. It is this effect which explains the high spin density at Cl^-_{IV}.

This is an interesting effect in view of the fact that the total charge transfer is only $-0.015|e|$ (e = proton charge). This may be typical for many centres showing weak covalency: the main effects of modest charge transfer may become apparent through the polarization of neighbouring ions. First estimates show that this effect can also explain the remaining discrepancies of the interstitial centres (27).

The ground state of atomic hydrogen seems pretty much understood now, although a calculation of the "covalency" (mixing) parameters from first principles is still missing. As it turned out it was not only the simple electronic structure of the hydrogen atom, which made it a model defect, but also its light mass with the resulting large vibrational amplitudes. The dynamical part of the shf constants for $H^o_{s,a}$-centres is up to 50%. Its calculation provided a very hard test for various theoretical models, since the distance dependence of all interactions had to be correctly understood.

3. Electronic structure of excited states

About the optically excited states far less is known and its understanding is still in a qualitative stage. No optical results are yet available for substitutional centres, which

restrict the discussion to the interstitial centres.

Interstitial centres have optical absorption bands between 3.5 and 5.5 eV. The absorption is due to charge transfer transitions, in which a halogen p electron goes over to the hydrogen atom forming H^- and leaving a hole in the halogens as discussed already above to explain the ground state. In most alkali halides the centres have several UV absorption bands. Magneto-optical measurements have shown that the transitions occur from the A_1 ground state to the two symmetry allowed $T_{2\sigma}$ and $T_{2\pi}$ linear combinations of the outer halogen p orbitals. These transitions are well resolved in the bromides and iodides (28,29,30).

Until recently no fluorescence emission was observed from interstitial centres except for one particular mixed configuration, in which one of the 4 nearest halogen neighbours is replaced by a I^- (see Fig. 7), but no emission was found if in a chloride one halogen neighbour was Br^-. It seemed that I^- was responsible, although in pure KI no emission was observed.

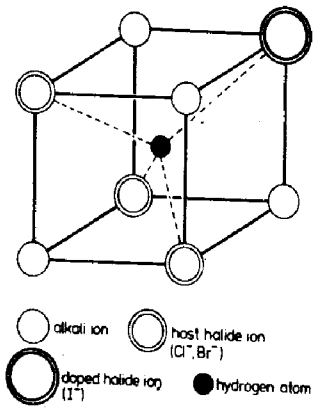

Fig. 7:
Model of interstitial hydrogen centres in the mixed configuration with one I^- next (H_i^o(I)-centres)). (After [38]).

The first luminescence of "pure" interstitial hydrogen centres was found in the Cs-halides, where the symmetry of the centres is different from those in the NaCl type alkali halides. In CsBr, e.g., an emission band was found at 1.11 eV. Fig. 8 shows absorption, excitation spectrum and magnetic circular dichroism (MCD). From the latter two it is clear that 3 absorption bands exist. The Stokes shift is with approximately 3.5 eV very large. The 3 bands can be qualitatively understood with a simple charge transfer model, in which the outer p hole states are split by the spin orbit interaction of Br^o and the difference in Coulomb

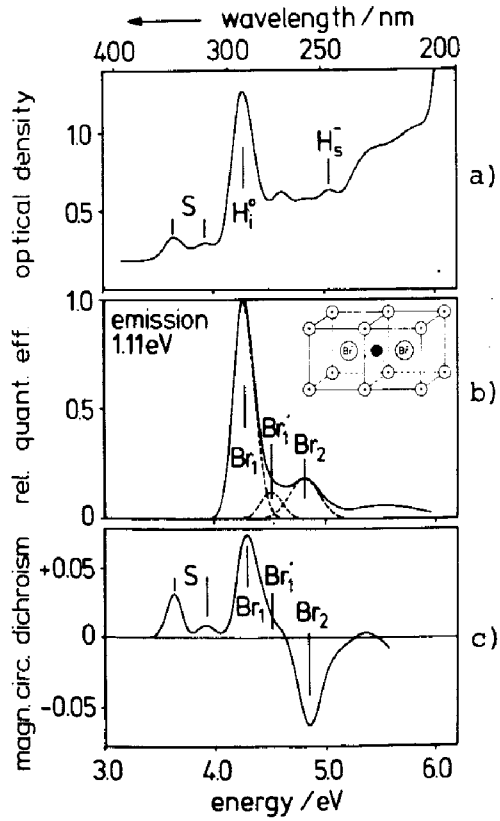

Fig. 8:
Interstitial centres in CsBr.

a) Optical absorption
b) Excitation spectrum for the emission at 1.11 eV.
c) Magnetic circular dichroism (MCD).
(After [31]).

interaction between H^- and p_σ and p_π hole orbitals, the direction being the connection line between Br^o and H^- ([100]) (31).

Very recently it was possible to detect also the emission of interstitial centres in KI at 0.91 eV (Fig. 9b). The absorption and the excitation spectrum agrees very well. The measurement was made possible by the use of a highly sensitive Ge IR detector in the range between 0.7 and 1.5 eV (North Coast Eo-817) (32). The emissions of halogen centres are very weak and their detection has been delayed by the very large Stokes shift which brings them to an experimentally unfavourable wave length range. In competition to the emission the hydrogen centres decay upon optical excitation forming U centres (H_s^--centres) and "H-centres" (Halogen$_{2s}^-$-centres) (33,34) in a process analogous to the fundamental process of F and H-centre formation from a relaxed state of the self trapped exciton (35). An interesting feature was the observation that upon bleaching hydrogen centres at low temperatures with polarised UV light H-centres were produced in preferential orientations. Their axes were

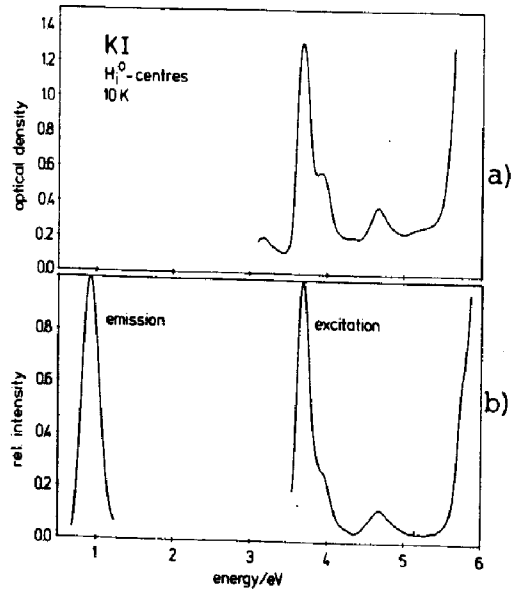

Fig. 9:
Interstitial centres in KI.
a) Optical absorption.
b) Excitation spectrum for the emission at 0.91 eV and emission band.

perpendicular to the E-vector of the exciting light, that is perpendicular to the direction of the charge transfer absorption moment. This suggested that the H centres were formed in an excited π-state (36).

Since very recently a more detailed information is available about the relaxed excited state of hydrogen centres, because it was possible to measure the optically detected magnetic resonance (ODMR) of one excited state for hydrogen in the mixed configuration, where one halogen neighbour is replaced by I^- (see Fig. 7). The structure of those H_i^o(I)-centres was established by ESR (37). The optical properties of those centres are shown in Fig. 10 for H_i^o(I)-centres in RbCl. There are several absorption bands in the UV, in which 2 fluorescence emission bands at 2.03 eV ("red") and 2.91 eV ("blue") can be excited. As seen from the MCD measurements there is a large spin orbit effect in the unrelaxed excited state, which can only be due to iodine (3/2 λ of free I^o = 0.944 eV, 3/2 λ of free Cl^o = 0.1 eV). It follows that the three low energy absorption bands are "iodine-like" and can be explained in a similar way as described above for H_i^o-centres in CsBr. The high energy band is due to "chlorine-like" charge transfer transitions. A particularly interesting feature of the optical properties of those mixed centres is the fact, that there are two red emission bands superimposed one of which has a radiative life time of

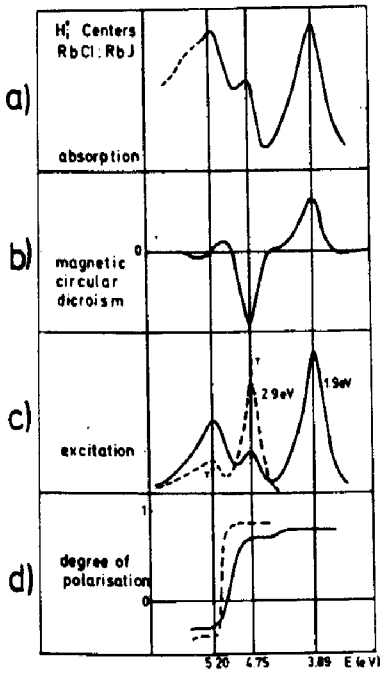

Fig. 10:
Interstitial centres in the I^- mixed configuration in RbCl (H_i^o(I)-centres)).

a) Optical absorption.
b) Magnetic circular dichroism.
c) Excitation spectrum of the blue and red emission.
d) Degree of polarisation of the emission as function of the excitation wave length.

31 nsec (the blue emissions have similar life times) and the other one of 370 nsec at 4 K (for KCl : 14 and 720 nsec, respectively). The optical properties are summarized in the level scheme of Fig. 11 (39). The state with the long radiative life time was proposed to be a spin quartet state in analogy to the triplet state of the self trapped exciton. In this state the two electrons at H^- and the hole at I^o have parallel spins. The long life time of this state seemed favourable to perform ODMR experiments in order to check the qualitative interpretation of the optical properties and to get more detailed information about this state.

ODMR experiments could be performed successfully only very recently and therefore only first results can be reported here (40).

The experimental method used was first applied to F-centres (41). The centres were pumped in the low energy absorption band (with a Xenon lamp and monochromator) with light having modulated polarisation and the ODMR was detected as a change in the MCD signal of the absorption under the influence of a cw microwave radiation. Fig. 12 shows the X-band spectrum for $B_o \| [100]$ obtained with this method for KCl. The same spectrum

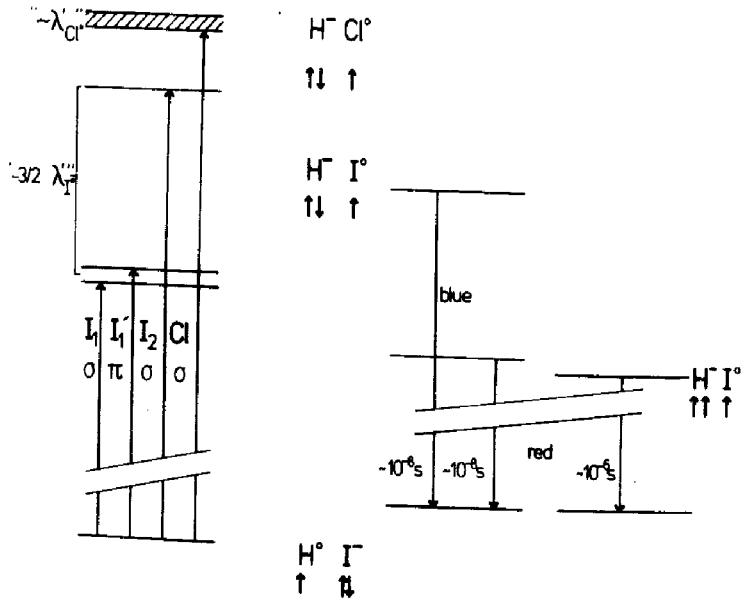

Fig. 11:

Schematic representation of the energy levels and optical properties of H_i^o(I)-centres in KCl and RbCl. (After [39]).

is also obtained if one observes the σ_+ or σ_- circular polarised light of the red emission instead of the MCD signal of the absorption. No signal was obtained if one observes the circular polarisation of the blue emission. In the upper part of Fig. 12 the conventional ESR spectrum of the ground state is shown for comparison with its analysis: the proton hyperfine and the iodine superhyperfine structure (nuclear spin of ^{127}I = 5/2) as well as the ODMR spectrum contains also the ground state signals at the same field positions and with the same splittings. Only the Cl shf interaction could not be resolved, since the homogeneity of the split coil superconducting magnet used (5 T-magnet) was not good enough for that. In between the ground state lines new lines appear which are due to the relaxed excited state. They show a different dependence on the microwave power compared to those of the ground state - at lower microwave power they disappear. It was surprising to find the lines of the excited state right in the middle between the ground state lines. Since in the conventional ESR spectrum there are no forbidden transitions, it was hard to believe that the new lines could be due to forbidden transitions, which would occur there. Measurements of the ODMR in K band confirmed that these lines are not due to forbidden transitions, since there the ratio between the new lines and those of the ground

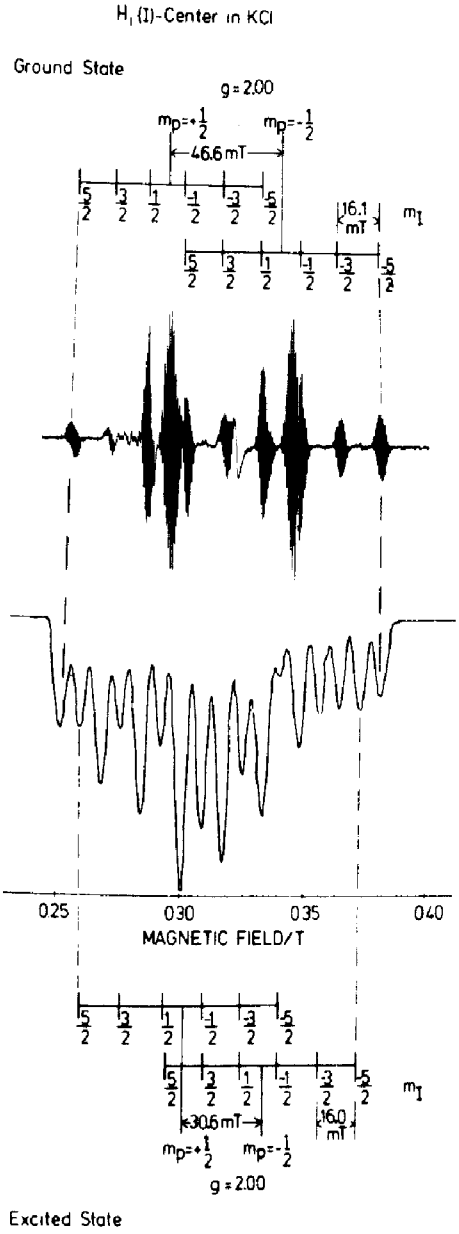

Fig. 12:

ESR spectrum of the ground state and ODMR spectrum of the ground and excited state of H_i^o(I)-centres in KCl. $B_o \parallel [100]$, ν = 9.4 GHz. T = 1.6 K. (After [40]).

state was exactly the same as in X-band, which could not be the case for forbidden lines (42,43,44).

The angular dependence could be measured, but not yet fully analysed. However, the symmetry of the excited state spectrum is also (111). Table 2 summarizes the results obtained. From the present experiments and the analysis up to now in KCl and RbCl the following properties of the excited state can be stated:

i) Up to magnetic fields of 5 Tesla no level crossing of the spin quartet could be observed in the magnetic circular polarisation of the emission (MCPE). Therefore, the quartet must be split by a very large zero field

splitting into two independent Kramers doublets, ODMR is observed in the doublet $m_s = \pm \frac{1}{2}$.

ii) The g-factors of the ground and excited state are practically the same.

iii) From the observed value of the proton hyperfine constant can be concluded qualitatively that indeed a spin quartet state was observed. For a doublet state the value of the proton hyperfine constant should only be a few Gauss.

iv) The spin mixing parameter ε (40) must be rather large, since with comparatively weak light intensity it was possible to pump the centres. The experiment suggests, that there is only one spin mixing parameter.

v) A preliminary analysis of the proton hyperfine interaction shows that in the relaxed charge transfer state the electron at the hydrogen is in a 2s-like state.

Table 2

Hyperfine and superhyperfine data of $H_i^o(I)$-centres in the ground and excited state

	Ground state*			Excited state		
	$g_{[100]}$	a_p[G]	Δ_I[G]	$g_{[100]}$	a_p[G]	Δ_I[G]
KCl	2.002	466	161	2.00	306	160
RbCl	2.003	462	153	2.00	308	152

* After [37].

Δ_I is the splitting of the I-superhyperfine levels for $B_o \| [100]$.

$\Delta = \sqrt{a^2 + 2b^2}$.

With the possibility to perform ODMR experiments and possibly also ENDOR measurements with optical detection it will be possible to describe the relaxed excited state in more detail and perhaps with a quantitative understanding as for the ground state. From our experiments it seems not unlikely, that also the ODMR of "pure" H_i^o-centres can be measured.

In summary it may be remarked that hydrogen centres promise to become perhaps those centres whose electronic structure in both ground and excited states can be quantitatively understood with a comparatively simple theoretical model.

1) J.M. Spaeth, J. de Physique C9, 267 (1972)

2) B.J. Delbecq, B. Smaller, and P.H. Yuster, Phys.Rev. 104, 599 (1956)

3) F. Kerkhoff, W. Martienssen, and W. Sander, Z.Physik 173, 184 (1963)

4) F. Fischer and H. Gründig, Z.Physik 184, 299 (1965)

5) F. Fischer, Z.Physik 187, 262 (1965)

6) Ch. Hoentzsch, and J.M. Spaeth, phys.stat.sol.(b) 88, 581 (1978)

7) P. Studzinski, J.R. Niklas, and J.M. Spaeth, phys.stat. sol.(b) 101, 673 (1980)

8) W. Hayes and J.W. Hodby, Proc.Roy.Soc. A 294, 359 (1966)

9) L. Schwan, Dissertation, Stuttgart 1975

10) H. Pick, Einführung in die Festkörperphysik, Wiss.Buchgesellschaft, Darmstadt 1978

11) G. Heder, J.R. Niklas, and J.M. Spaeth, phys.stat.sol.(b) 100, 567 (1980)

12) J.M. Spaeth, Z.Physik 192, 107 (1966)

13) M. Sturm and J.M. Spaeth, phys.stat.sol. 42, 739 (1970)

14) M.H. Wagner and J.M. Spaeth, Solid State Commun. 14, 1101 (1974)

15) J.M. Spaeth and H. Seidel, phys.stat.sol.(b) 46, 323 (1971)

16) Ch. Hoentzsch and J.M. Spaeth, phys.stat.sol.(b) 94, 497 (1979)

17) J.M. Spaeth, phys.stat.sol. 34, 171 (1969)

18) E. Goovaerts, L. de Schepper, A. Bouwen, and D. Schoemaker, phys.stat.sol.(a) 59, 597 (1980)

19) W. Kuch, Diplomarbeit, Stuttgart 1977

20) G. Heder, J.R. Niklas, and J.M. Spaeth, to be published

21) G. Heder, Dissertation, Paderborn, 1979

22) A.B. Lidiard and M.J. Norgett, Computational Solid State Physics ed F. Herman et al. (N.Y. Plenum) (1972)

23) C.R.A. Catlow, M.K. Diller, and M.J. Norgett, J.Phys.C: Solid State Phys. 10, 1395 (1977)

24) G. Heder, J.M. Spaeth, and A.H. Harker, J.Phys.C 13, 4965 (1980)

25) K. Cho, J.Phys.Soc. Japan 23, 1296 (1967)
26) K. Cho, H. Kamimura, and Y. Uemura, J.Phys.Soc.Japan 21, 2244 (1966)
27) A.N. Jette and F.J. Adrian, private communication
28) B.C. Cavenett, J.V. Gee, W. Hayes, and M.C. O'Brian, Solid State Commun. 6, 697 (1968)
29) J. Ingels and G. Jacobs, phys.stat.sol. 45, 107 (1971)
30) J.V. Gee, W. Hayes, and M.C. O'Brian, Proc.Roy.Soc. A 322, (1971)
31) Th. Hangleiter and J.M. Spaeth, Solid State Commun. 35, 23 (1980)
32) Th. Hangleiter and J.M. Spaeth, to be published
33) G. Kunz, phys.stat.sol. 31, 93 (1969)
34) G. Reuter, L. Schwan, and J.M. Spaeth, phys.stat.sol.(b) 53, K 29 (1972)
35) N. Itoh and A.M. Stoneham, J.Phys. C 10, 4197 (1977)
36) G. Reuter, F. Lohse, and J.M. Spaeth, phys.stat.sol.(b) 96, 243 (1979)
37) L.O. Schwan, H.J. Paus, R. Bauer, and J.M. Spaeth, Semiconductors and Insulators 5, 91 (1980)
38) F. Lohse, G. Reuter, and J.M. Spaeth, phys.stat.sol.(b) 89, 109 (1978)
39) F. Lohse and J.M. Spaeth, phys.stat.sol.(b) 93, 153 (1979)
40) B. Meyer, F. Lohse, and J.M. Spaeth, to be published
41) L.F. Mollenauer and S. Pan, Phys.Rev. B 6, 772 (1972)
42) A. Abragam and B. Bleaney, Electron Paramagnetic Resonance of Transition Ions, Clarendon Press, Oxf. 1976
43) A. Hausmann and S. Köpp, Z.Physik 243, 373 (1971)
44) J.L. Hall and R.T. Schumacher, Phys.Rev. 127, 1892 (1962)